



# Quantifying the Regional Water Balance of the Ethiopian Rift Valley Lake Basin Using an Uncertainty Estimation Framework

Tesfalem Abraham<sup>1,2\*</sup>, Yan Liu<sup>2</sup>, Sirak Tekleab<sup>1</sup>, Andreas Hartmann<sup>2,3</sup>

<sup>1</sup>Department of Water Resources and Irrigation Engineering, Institute of Technology, Hawassa University, Hawassa, Ethiopia

<sup>2</sup>Faculty of Environment and Natural Resources, University of Freiburg, Freiburg, Germany

<sup>3</sup>Department of Civil Engineering, University of Bristol, Bristol, UK

Correspondence to: Tesfalem Abraham ([atesfalem@gmail.com](mailto:atesfalem@gmail.com))

**Abstract.** In Ethiopia more than 80 % of big freshwater lakes are located in the Rift Valley Lake Basin (RVLB), serving over 15 million people a multipurpose water supply. The basin covers an area of 53,035 km<sup>2</sup>, and most of the catchments recharging these lakes are ungauged and their water balance is not well quantified, hence limiting the development of appropriate water resource management strategies. Prediction for ungauged basins (PUB) has demonstrated its effectiveness in hydro-climatic data-rich regions. However, these approaches are not well evaluated in climatic data-limited conditions and the consequent uncertainty is not adequately quantified. In this study we use the Hydrologiska Byråns Vattenbalansavdelning (HBV) model to simulate streamflow at a regional scale using global precipitation and potential evapotranspiration products as forcings. We develop and apply a Monte-Carlo scheme to estimate model parameters and quantify uncertainty at 16 catchments in the basin where gauging stations are available. Out of these 16, we use the 14 most reliable catchments to derive the best regional regression model. We use three different strategies to extract possible parameter sets for regionalization by correlating the best calibration parameters, the best validation parameters, and parameters that give the most stable predictions with catchment properties that are available throughout the basin. A weighting scheme in the regional regression accounts for parameter uncertainty in the calibration. A spatial cross-validation is applied multiple times to test the quality of the regionalization and to estimate the regionalization uncertainty. Our results show that, other than the commonly used best-calibrated parameters, the best parameter sets of the validation period provide the most robust estimates of regionalized parameters. We then apply the regionalized parameter sets to the remaining 35 ungauged catchments in the RVLB to provide regional water balance estimations, including quantifications of regionalization uncertainty. The uncertainties of elasticities from the regionalization in the ungauged catchments are higher than those obtained from the simulations in the gauged catchments. With these results, our study provides a new procedure to use global precipitation and evapotranspiration products to predict and evaluate streamflow simulation for hydro-climatically data-scarce regions considering uncertainty. This procedure enhances the confidence to understand the water balance of under-represented regions like ours and supports the planning and development of water resources.

**Keywords:** Parameter Estimation, Uncertainties, Ungauged Catchment, Weighted Regression, Water Balance

## 1 Introduction

Global freshwater is particularly stressed by the rapidly increasing human population and by all the negative consequences of environmental change. Hydrological quantification of freshwater resources is crucial to manage and mitigate these impacts, and consequently promote the benefits gained from the resources. As such, there is a growing need for accurate monitoring and simulation of water balance components to support and maximize water resource management practices. In Ethiopia most of



the freshwater lakes are bounded in the Great East African Rift Valley system, which was formed by volcanic depressions and cracks in the Pliocene age (Woldegabriel et al., 1990). The region is known for its scarce and limited hydro-climatic data, which has limited the regional understanding of water balance processes. In many developing regions in the world, hydro-climatic stations are not sufficiently established due to a limited amount of economic and technological development (Stokstad, 1999).

40 In the Ethiopian Rift Valley Lake Basin (RVLB), even the data in the few available gauging networks are of poor quality, contain gaps, and are subjected to human disturbances. Consequently, the region has remained one of the least studied regions in Ethiopia. Due to the data scarcity issue, there lacks hydrological simulations using available rainfall-runoff models in poorly managed catchments across the world. New approaches utilizing global datasets and quantifying uncertainties will be helpful for those data scarce regions.

45 The Prediction for ungauged basins (PUB) initiative aims in particular at developing strategies for increased understanding and reduced uncertainty in data-sparse regions (Blöschl et al., 2011; Sivapalan et al., 2003). Studies have started to focus on ungauged catchment predictions (Sivapalan et al., 2003; Wagener et al., 2004). Two general approaches have been used for predictions in ungauged basins; the first one estimates model parameters from the calibrated model parameters based on selected objective functions (Wagener and Wheater, 2006); the second is a model-independent approach, which uses

50 streamflow signatures to establish constraints that can describe the physical and climatic characteristics of watersheds (Wagener and Montanari, 2011). The latter has been shown to reduce uncertainties that can emerge from the model structural error (Bárdossy, 2007; Kapangaziwiri et al., 2012; Singh et al., 2013; Yadav et al., 2007; Zhang et al., 2008). Gauged watersheds with sufficient climatic data are used to develop regional relationships between the streamflow signatures and the catchment properties of watersheds. This approach has shown skill in predicting the expected streamflow in ungauged catchments

55 especially when going along with quantification of uncertainties emerging from observed streamflow data (Westerberg et al., 2016). But recent work also showed that the information content of streamflow signatures is limited (Addor et al., 2018). So far, however, most of these approaches have only been applied in data-rich regions of the world. The credibility and validity of such strategies have yet to be well tested in poorly recorded climatic data conditions.

Rainfall-runoff models are used to represent the typical physical and climatic properties of a catchment. The physical

60 representation of the available rainfall-runoff models may range from parsimonious-spatially lumped to complex physical-spatially distributed models. The common problem with most rainfall-runoff models is that they require some sort of parameter estimation to provide robust predictions. Most model parameters are not directly measurable or linkable to the physical properties of the given catchment because of model simplifications or disagreements between model scale and observation scale (incommensurability) (Beven, 2006, 2018). However, an inherent correlation between the model parameters and

65 catchment properties can often be assumed (Merz and Blöschl, 2004; Seibert, 1999; Wagener et al., 2004). Model parameters represent the characteristics of the complex catchment system, which are difficult to measure at a small scale. The accurate representation of catchment properties by the model parameters should be evaluated, to some degree, by the selected objective function that measures the fit between observed discharge and simulated discharge. However, most of the catchments are ungauged and their parameter estimations will be subject to uncertainties. Despite the aforementioned limitations in data-scarce

70 regions, there are some studies that have developed strategies to derive model parameters at the global scale using various regionalization approaches (Döll et al., 2003; Nijssen et al., 2001; Widén-Nilsson et al., 2007). Yet, the obtained simulations often show a lack of precision due to errors emerging from global input data quality and regionalization uncertainty. Uncertainties would be particularly propagated due to the regionalization method itself and the human interference in the



catchments (Widén-Nilsson et al., 2007). Another approach estimates regionalized parameter sets at a global scale by using  
 75 data from catchments mainly distributed in the temperate regions (Beck et al., 2016); their realization and validity in the tropics  
 remain under question since their regionalization procedure does not include many catchments from this climatic region.

In this study, we test the applicability of high-resolution global climate data for deriving a regional model and demonstrate a  
 novel spatial cross-validation procedure to quantify regionalization uncertainties for the region in the RVLB with scarce  
 precipitation data. Other than the typical approach of using the best-calibrated parameters of the gauged catchments (e.g.  
 80 Wagener and Wheeler, 2006), we extend the idea of using multiple similar parameter sets for regionalization (e.g., Livneh and  
 Lettenmaier, 2013) by using three different parameter sets. Using a spatial split-sample test, we evaluate the best-calibrated  
 parameter, the best parameter set in the validation period, and the most stable parameter set considering their performance in  
 calibration and validation period for their adequateness for regionalization. We implement this approach to a relatively low  
 number of 16 gauged catchments with reliable streamflow data to estimate the water balances of 35 ungauged catchments in  
 85 the RVLB. Repeating the spatial split-sample test multiple times, we quantify the uncertainty that goes along when  
 regionalizing parameter sets from a low number of catchments. That way, our study provides useful directions for regional  
 modeling and uncertainty quantification in under-represented and a data-sparse region like ours, where assessments of the  
 impacts of climate variability and climate changes are most urgently needed.

## 2 The study region

90 The RVLB is located in the southern part of the Main Ethiopian Rift (MER), which supplies water for a population of more  
 than 15 million, where subsistence agriculture is the main livelihood (Fig. 1). The RVLB is 84 km wide and adjacent to it there  
 are large, discontinuous Miocene-aged normal faults (Abebe, 2005; Pizzi et al., 2006; Wolfenden et al., 2004). Within the MER  
 there are a series of right-stepping, quaternary rift basins, which have faulted magmatic segments, extending about 20 km wide  
 and 60 km long, that are embryonic oceanic spreading centers. The central part of RVLB is formed by a Pliocene-aged faulted  
 95 caldera, caused by fractured volcano (Woldegabriel et al., 1990) around the Tikur Wuha catchment. Existing faults and  
 repeatedly formed ground cracks on the floor of the caldera have increased the permeability of the rocks. Within the basin,  
 several small-to-medium-sized catchments drain to eight freshwater lakes. For most of these catchments, there is a lack of  
 hydro-climatic data; what data is available contain gaps and are subject to human interventions. Over the past decades, the  
 RVLB has experienced major droughts and extreme flood events resulting from the variable nature of precipitation, making  
 100 prediction difficult (Segele and Lamb, 2005). This has resulted in an uncertain analysis of high and low flows, factors that are  
 important for quantifying the hydrological water balance components in this region.

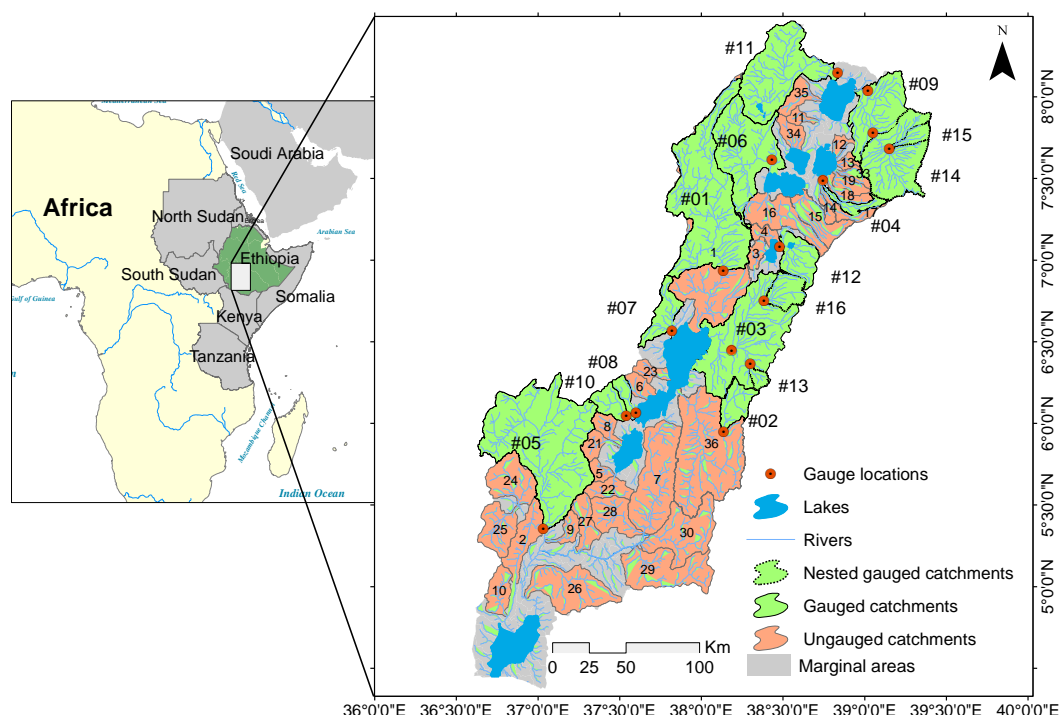


Figure 1: The study basin showing 16 gauged catchments for the regional model development and 33 ungauged catchments that are draining to the respective lakes through the river networks.

### 105 3 Methods and Data

We show the concept of the regionalization procedure in Fig. 2. We apply global parameter sets and climatic forcings for parameter estimation of gauged catchments using a hydrological model. We derive parameter sets that perform best during calibration and validation respectively, and ones that are stable between calibration and validation (stable parameter sets). Using the best parameter sets from calibration, we conduct a correlation analysis with the physical and climatic properties of catchments, which forms the basis for our regression. By applying the best parameters from calibration, validation, and stable sets, we derive regression models to estimate parameters for the ungauged catchments. In addition, we quantify the regionalization uncertainty through the spatial cross-validation procedure that applies the Leave-One-Out method. We then evaluate parameters derived from the regression by comparing discharge observations and simulations of the gauged catchments during their validation periods. This procedure enables the selection of the best regional models derived from the parameters estimated from calibration, validation, and stable sets.

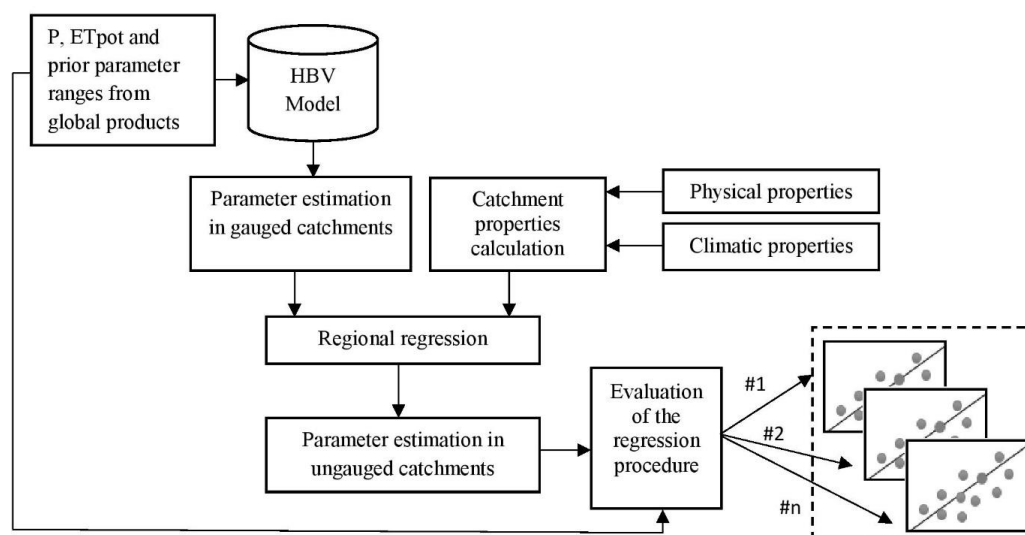


Figure 2: Schematic diagram showing the entire procedure applied in this study.

### 3.1 Data and catchment properties

In our regionalization procedure we use precipitation products of Multi-Source Weighted-Ensemble Precipitation (MSWEP) version 2 and evapotranspiration from the Global Land Evaporation Amsterdam Model (GLEAM V3) respectively (Table 1). MSWEP products have recently developed precipitation datasets at a finer scale (0.1°), which are constructed using different sets of precipitation data from gauges, monthly satellite data, and re-analysis data on the global scale. We collect the daily streamflow data for the period from 1995 to 2007 from the Ministry of Water Irrigation and Energy of Ethiopia (MOWIE) for 16 catchments in the RVLB, whose size ranges from 144.2 to 4,528.2 km<sup>2</sup>. The 16 catchments provide a sufficient length of data (>10 years) for the simulation periods. Of these, four catchments are nested within another catchment because they adequately satisfy the catchment selection criteria.

Table 1: Variables showing the climatic and physiographic data and their resolutions and periods.

Variable	Spatial resolution	Time period	Temporal resolution	Source	Reference
Precipitation	0.1°	1995–2007	Daily	MSWEP V2	Beck et al. (2019)
Potential evapotranspiration	0.25 °	1995–2007	Daily	GLEAM v3	Martens et al. (2017)
HBV-parameters	0.5 °	-	-	<a href="http://www.gloh2o.org">www.gloh2o.org</a>	Beck et al. (2016)
Elevation	30 m	-	-	SRMT V2.1	<a href="https://earthexplorer.usgs.gov">https://earthexplorer.usgs.gov</a>
Wetness index (P/PE)	Point scale	1995–2007	Daily	MSWEP V2 & GLEAM v3	Beck et al. (2019); Martens et al. (2017)
Streamflow	-	1995–2007	Daily	MOWIE	-

Catchment properties are common descriptors of the hydrological process and are frequently applied to estimate model parameters in ungauged catchments. However, there is no general rule to select suitable properties. The available option should be a selection of as many catchment descriptors as possible, while reducing correlated catchment properties so as to exclude



redundant information and obtain independent variables. In this regard, the main criteria to select catchment properties is that they are model-independent and can be used for model predictions to be hydrologically realistic in both gauged and ungauged catchments (Wagener and Montanari, 2011). For reliable regionalization, a sufficient number of catchment properties should  
135 be selected. Their selection, in turn, depends on data availability, hydrologic relevance, and the suitability of the properties. With these considerations, we derived nine catchment properties from the physical and/or climatic information in both gauged and ungauged catchments from the RVLB (Table 2 and Table S2). We extract physical catchment properties from the Digital Elevation Model (DEM), and climatic properties from the global data sets that usually affect the catchment hydrology in any setup. Other physical properties where local information is not available, such as permeability and porosity, were extracted  
140 from the global datasets prepared by Huscroft et al. (2018).



Table 2: Descriptions and values of properties for gauged catchments in the RVLB that were used for the development of the regional model.

Cat No and Names at the gauge location	Catchment properties	Drainage area [km <sup>2</sup> ]	Drainage density [km km <sup>-2</sup> ]	Mean Slope [%]	Mean elevation [m]	Catchment index [m km <sup>-1</sup> ]	Permeability [log <sub>10</sub> m <sup>2</sup> ]	Porosity [-]	Wi [-]	P [mm]
	Description of properties	Index of catchment area	The ratio of catchment stream length to the drainage area	Mean of the percentage slope for each terrain unit	Index describing the mean of catchment elevation	Mean of all inter-nodal slopes in a catchment	Index describing the nature of water flow in the shallow aquifer	The fraction of the volume of voids in the shallow aquifer	Wetness index (Wi) as the ratio of precipitation (P) to potential evapotranspi- ration (PE)	Annual average precipitation (1995– 2007)
#01-Bilate@Tena		3821.2	0.075	16.22	2037.1	10.07	-12.194	0.07	0.85	923.6
#02-Gelana@Tore bridge		506.4	0.124	24.17	2084.5	10.39	-12.5	0.09	1.17	1309.1
#03-Gidabo@Measso		2590	0.113	20	1805.4	14.54	-12.248	0.097	0.85	942.07
#04-Gedemso@Langano		241.5	0.67	18.1	2759.3	28.11	-12.5	0.09	0.88	919.19
#05-Woito@Bridge		4528.2	0.07	29.09	1439.5	10.64	-11.433	0.028	1.34	1319.6
#06-Djido@Hitsanat amba		2062.2	0.116	13.88	1933.8	4.41	-12.035	0.068	0.68	737.6
#07-Hamassa@Wajifo		534.4	0.34	15.86	1655.5	15.22	-12.306	0.076	0.94	1208
#08-Hare		196.5	0.36	33.08	2343.1	77.67	-12.2	0.076	0.897	1107.5
#09-Katar@Abura		3241.1	0.115	8.7	2601.9	19.99	-12.034	0.064	0.69	779.8
#10-Kulfo@Arbaminch		397.2	0.226	36.39	2249.9	76.55	-12.283	0.08	1.52	1617.8
#11-Meki@Meki village		2033.1	0.111	19.27	2124.4	11.12	-12.155	0.068	0.58	667.2
#12-Tikur wuha@Bridge		631.3	0.308	12.12	2085.6	16.37	-11.885	0.05	1.09	1128.3
#13-Gidabo@Bedesa*		144.2	0.341	30.18	2149.7	56.74	-12.5	0.09	1.29	1397.7
#14-Katar@Fete*		1940.9	0.117	14.49	2668.9	17.78	-12.171	0.075	0.87	991.2
#15-Katar@Timela*		205.2	0.65	18.29	2953.5	40.87	-12.371	0.084	0.7	785.6
#16-Gidabo@Aposto*		491.8	0.327	21.49	2012.6	26.76	-12.483	0.089	1.18	1300.1

\*Nested gauged catchments that overlap with another gauged catchment used for the regionalization procedure.



### 3.2 Hydrological model

We use the lumped HBV hydrologic model (Bergström, 1992; Seibert and Vis, 2012), which has been applied in a wide range of climatic and physiographic conditions (Te Linde et al., 2008; Zhang and Lindström, 2007). The HBV model has been tested in various parts of the world and frequently applied in several regionalization studies due to the simplicity and flexibility of its model structure (Bárdossy, 2007; Hundecha and Bárdossy, 2004; Jin et al., 2009; Masih et al., 2010; Merz and Blöschl, 2004; Parajka et al., 2007; Seibert, 1999).

In this study we apply the HBV model modified by Zhang and Lindström, (2007) and Beck et al. (2016). We run the model at a daily time scale using daily inputs of precipitation and potential evapotranspiration. Due to the absence of snow processes in the RVLB, the model we use consists of routines of soil moisture accounting, runoff response, and a channel routing procedure, which are controlled by nine model parameters (Table 3). Three parameters,  $\beta$ ,  $F_C$ , and  $L_P$ , control the soil moisture dynamics.  $\beta$  controls the contribution ( $dQ$ ) to the runoff response routing and the increase ( $dP-dQ$ ) in soil moisture storage ( $S_{sm}$ ) and  $F_C$  is the maximum soil moisture storage in the model as shown by Eq. (1).  $L_P$  is the value of the soil moisture above which evapotranspiration ( $E_a$ ) reaches its potential level ( $E_p$ ).

$$\frac{dQ}{dP} = \left(\frac{S_{sm}}{F_C}\right)^\beta \quad (1)$$

Where  $P$  and  $Q$  are precipitation and runoff [ $\text{mm d}^{-1}$ ].

The runoff response function transforms excess water from the soil. This routine consists of upper and lower reservoirs that distribute the generated runoff over time. The lower reservoir is a simple linear reservoir representing a contribution to baseflow. It also includes the effects of direct precipitation and evaporation over open water bodies in the basin. The lower reservoir storage,  $S_{LZ}$  [mm], is filled by percolation from the upper reservoir ( $P_{MAX}$ ), and the outflow from this lower reservoir ( $Q_2$ ) is controlled by the recession coefficient  $K_2$  [ $\text{d}^{-1}$ ]. However, the upper reservoir storage  $S_{UZ}$  [mm] is drained by two recession coefficients,  $K_0$  [ $\text{d}^{-1}$ ] and  $K_1$  [ $\text{d}^{-1}$ ], draining the quick flow  $Q_0$  [ $\text{mm d}^{-1}$ ] and slow flow component  $Q_1$  [ $\text{mm d}^{-1}$ ] separated by a threshold  $V_{UZL}$  [mm] Eq. (2–4).

$$Q_0 = K_0(S_{UZ} - V_{UZL}) \quad (2)$$

$$Q_1 = K_1(S_{UZ}) \quad (3)$$

$$Q_2 = K_2(S_{LZ}) \quad (4)$$

If the yield  $dQ$  [ $\text{mm d}^{-1}$ ] from the soil moisture routine exceeds the capacity, the upper reservoir will start to fill. This reservoir models the response at flood periods. Parameters calibrated from the runoff response function are  $P_{MAX}$ ,  $K_0$ ,  $K_1$ ,  $K_2$ , and  $V_{UZL}$ . Finally, runoff is computed independently for each sub-basin by adding the contributions from the upper and the lower reservoir. To account for the damping of the flood pulse in the river before reaching the basin outlet, a simple routing transformation is made. This filter has a triangular distribution of weights with the base length and is expressed by the parameter  $M_{MAXBAS}$  [d]. A detailed description of the model is shown by Bergström (1992) and Seibert and Vis (2012). The ranges of the nine model parameters are derived from prior knowledge, provided through a global set of HBV model parameters (Beck et al., 2016).





Table 3: HBV parameter ranges for the RVLB and their descriptions, derived from Beck et al. (2016).

Parameter	Description	Global range (min to max)
$\beta$ [-]	Shape coefficient of recharge function	1–6
$F_C$ [mm]	Maximum water storage in unsaturated-zone store	50–700
$K_0$ [ $\text{d}^{-1}$ ]	Additional recession coefficient of upper groundwater store	0.05–0.99
$K_1$ [ $\text{d}^{-1}$ ]	Recession coefficient of upper groundwater store	0.01–0.8
$K_2$ [ $\text{d}^{-1}$ ]	Recession coefficient of lower groundwater store	0.001–0.15
$L_P$ [-]	Soil moisture value above which actual evaporation reaches potential evaporation	0.3–1
$M_{MAXBAS}$ [d]	Length of equilateral triangular weighting function	1–3
$P_{MAX}$ [ $\text{mm d}^{-1}$ ]	Maximum percolation to lower zone	0–6
$V_{UZL}$ [mm]	Threshold parameter for extra outflow from upper zone	0–100

### 3.3 Parameter estimation in the gauged catchments

We use a uniform random sampling strategy to produce simulated streamflow ensembles with the HBV model. To obtain reasonable parameter sets, we generated 20,000 combinations of the 9 HBV parameters from a uniform random Monte-Carlo sampling procedure. We use a split sample test (Klemeš, 1986) by splitting the simulation period into the calibration period (1995–2002) and the validation period (2003–2007), and calculate the Nash Sutcliffe Efficiency (NSE) (Nash and Sutcliffe, 1970) for both periods:

$$NSE = 1 - \frac{\sum_{i=1}^n (Q_{obs} - Q_{sim})^2}{\sum_{i=1}^n (Q_{obs} - \bar{Q}_{obs})^2} \quad (5)$$

Where  $Q_{obs}$  and  $Q_{sim}$  are monthly averages of observed and simulated discharges [ $\text{m}^3 \text{month}^{-1}$ ], respectively, while  $\bar{Q}_{obs}$  is the mean observed discharge over the calibration or validation periods. Using monthly averages, we focus on the seasonal, long-term behavior instead of daily, short-term fluctuations. In order to remove unrealistic parameter combinations, we only kept parameter sets that produced  $NSE \geq 0.5$  in the calibration period. Consequently, different catchments can result in a different number of behavioral parameter sets. A pre-analysis using NSE on a daily time scale showed that the model performs well for all but two catchments (#06 and #12), where the fast flow processes and the occurrence of wetlands respectively resulted in poor simulations. Thus, these catchments are omitted in the following analysis. Comparing the mean and variability of model performance for the remaining catchments during calibration and validation allows to assess the predictive performance and uncertainty of the selected parameter sets. To prepare for regionalization, we extract (1) the variability of each model parameter in the reduced parameter sample (expressed by their coefficient of variation, CV), and (2) the best parameter set (largest NSE) of the calibration,  $NSE_{CAL}$ , and the validation period,  $NSE_{VAL}$ , for each of the catchments. In addition, we identify the most stable parameter set for each catchment, i.e., the parameter set that shows the smallest difference of NSE values between calibration and validation periods,  $NSE_{DIFF}$ :

$$NSE_{DIFF} = \min |NSE_{CAL} - NSE_{VAL}| \quad (6)$$

### 3.4 Parameter estimation in the ungauged catchments

To estimate model parameters for the 35 ungauged catchments, we develop a parameter regionalization procedure using weighted linear regressions (Eq. 7-9), also known as weighted least squares, and the non-linear regressions (Eq. 10). This



allows us to link the catchment properties (Table 2) and the estimated model parameters of the gauged catchments (*Sect 3.3*). Compared to the ordinary least squares, the weighted linear regression introduces a weight matrix to account for the unequal variances of observations (Tasker, 1980; Wagener and Wheeler, 2006). This brings advantages in the regionalization since the identifiability of a model parameter can vary significantly between catchments. To get a robust regression model, we can then  
 205 put more weights on catchments with identifiable parameters. The weighted linear regression is described as follows:

$$\mathbf{Y} = \mathbf{X}\boldsymbol{\beta} + \boldsymbol{\varepsilon} \quad (7)$$

$$\mathbf{W} = \begin{bmatrix} w_1 & 0 & \cdots & 0 \\ 0 & w_2 & \cdots & 0 \\ \vdots & \vdots & \ddots & \vdots \\ 0 & 0 & \cdots & w_n \end{bmatrix} \quad (8)$$

$$\hat{\boldsymbol{\beta}} = \underset{\boldsymbol{\beta}}{\operatorname{argmin}} \sum_{i=1}^n \varepsilon_i^2 = (\mathbf{X}^T \mathbf{W} \mathbf{X})^{-1} \mathbf{X}^T \mathbf{W} \mathbf{Y} \quad (9)$$

where  $\mathbf{Y}$  and  $\mathbf{X}$  are, respectively, the response variable (estimated model parameters in our study) and the independent variable  
 210 (catchment properties in our study).  $\boldsymbol{\varepsilon}$  is the error vector and  $\mathbf{W}$  is a diagonal matrix containing weights.  $\boldsymbol{\beta}$  represents the regression coefficients vector and is estimated by  $\hat{\boldsymbol{\beta}}$ , which minimizes the weighted sum of errors. The coefficient of variation (CV) of behavioral parameter sets of a catchment represents the variability of a parameter. The smaller the CV, the less variable and more identifiable the parameter. Therefore, we use the reciprocal CV of the parameter of interest as weights for each catchment. We perform the correlation analysis between model parameters and catchment properties to select independent  
 215 variables. We apply the linear correlation, Spearman's rank correlation (Spearman, 1904), and the correlation on the log-transformed scale. We select those properties with strong correlations to parameters according to the correlation coefficients. We also apply the non-linear regression between model parameters and catchment properties (Wagener and Wheeler, 2006).

$$Y = \beta_1 * X_i^{\beta_2} \quad (10)$$

where  $\beta_1$  and  $\beta_2$  are the regression coefficients. From the weighted linear regression and the non-linear regression, we choose  
 220 the catchment properties with the strongest correlation with the model parameter as the independent variable.

### 3.5 Evaluation and uncertainty estimation of the regionalization procedure

We use the Leave-One-Out method (Breiman and Spector, 1990) for parameter estimation and for evaluating the prediction skill of the regressions. Leave-One-Out is a simple cross-validation procedure: each regression model is created by taking all the catchments except one, the evaluation catchment. This method is more stable and resilient to errors emerging during  
 225 parameter sampling, and provides a comprehensive evaluation of prediction skills (Hastie et al., 2005). It has been applied for regionalization studies involving the prediction of discharge signatures using different regression techniques (Zhang et al., 2018). Thus, for 14 catchments we have 14 different regression models and 14 different evaluation catchments. For each of the 14 iterations, the method produces one regionalized model parameter set for the left-out catchment using the regression model derived from the remaining 13 catchments and parameter sets. Since we do not know which parameter sets provide the most  
 230 stable regionalization method, we repeat this procedure three times using the best parameter sets of (1) the calibration period, (2) the validation period, and (3) the most stable parameter sets between calibration and validation period. We thus evaluate the quality of the regionalization procedure three times. In order to choose the best of them for the following analyses, we evaluate the simulations of the left-out catchments for the validation phase (2003–2007). In order to quantify the uncertainty



of the regionalization procedure, we apply all 14 regionalized models that were created for the Leave-One-Out evaluation to the ungauged catchments. Hence, an ensemble of 14 predicted streamflow time series is produced for each ungauged catchment to reflect the regionalization uncertainty.

### 3.6 Estimation of regional resilience of streamflow to precipitation variability

In addition to the simulations at the 14 gauged catchments (and their respective uncertainty), our regionalization procedure produces simulations, and uncertainty estimates, of the 35 ungauged catchments, altogether covering a majority of the RVLB area (60.81 %). We use this regional simulation tool to estimate the region's streamflow resilience to precipitation variability, which we quantify through streamflow elasticity (Sankarasubramanian et al., 2001). The elasticity of streamflow quantifies the sensitivity of a catchment's streamflow response to the precipitation changes at the annual scale. Resilient catchments show low streamflow variability in response to precipitation changes. Elasticity is defined as the ratio between change in annual aggregated discharge ( $Q$ ) and change in annual aggregated precipitation ( $P$ ):

$$\varepsilon P = \text{median}\left(\frac{dQP}{dPQ}\right) \quad (11)$$

We calculate elasticity values for each year using the entire ensemble of simulated discharge time series at all gauged and ungauged catchments. From this we extract the median, wettest, and driest year elasticities for each catchment, including their uncertainty expressed by the respective CV resulting from all parameter sets with  $\text{NSE} \geq 0.5$  for the gauged catchments and from the 14 parameter sets obtained through the Leave-One-Out procedure for the ungauged catchments. The wettest year elasticity is calculated for the transition from the normal year to the wettest year, and the driest year elasticity is calculated for the transition from the normal year to the driest year. Using the median, wettest, and driest year elasticities, we can learn how resilient a hydrological system is against extreme climatic conditions such that we can evaluate the corresponding security for water supply. For instance, if a catchment has a large streamflow elasticity, there will be a large system change in response to a big change in precipitation (e.g., the driest year); such a system is not resilient as there would be a huge change in the water available, thus affecting the security of the water supply.

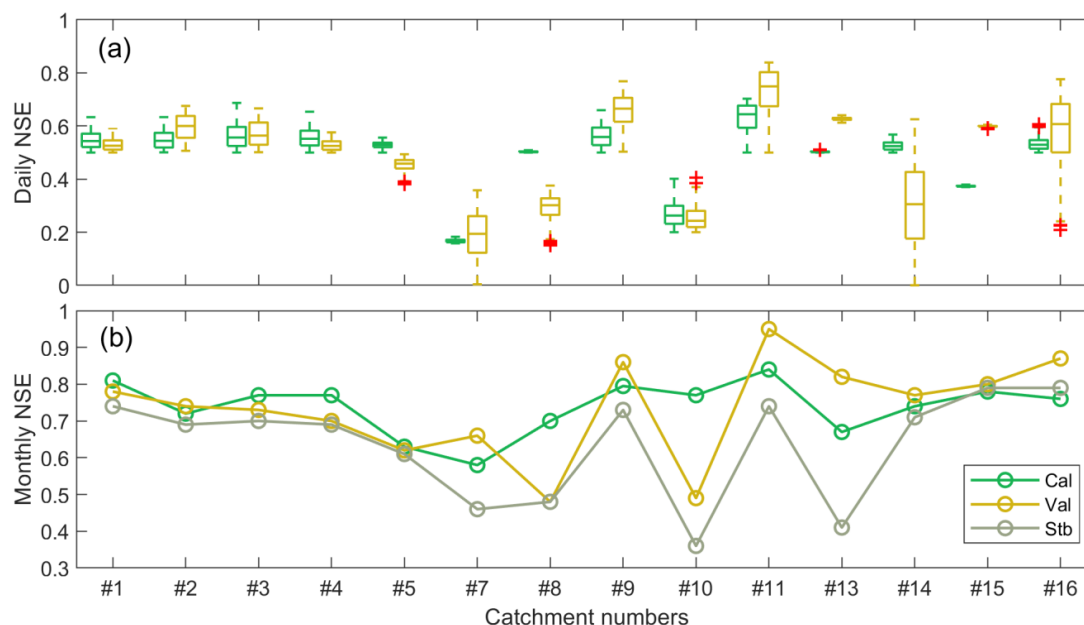
## 4 Results

### 4.1 Estimated parameters in the gauged catchments

Using the 0.5 NSE threshold, we obtain a wide range of behavioral parameter sets in all gauged catchments. Figure 3a shows the daily values of NSE for the calibration and validation periods, as well as their uncertainty, using behavioral parameter sets. For monthly calibrations, model performance results in NSE 0.58 to 0.84, except for catchments #06 and #12, which performed poorly and were considered ungauged for the following analysis. The change of NSE values from the calibration to the validation periods were reduced for catchment #08 and #10 (Fig. 3b). Catchments #01, #03, and #04 show a small decrease in the monthly NSE values from the calibration to the validation period (Fig. 3b). In most cases, the monthly model calibration and validation show a uniform distribution of NSE values, indicating the stability of model parameters. NSE values for the stable parameter set shows the maximum value (0.79) for catchments #15 and #16, demonstrating good predictive skills in these catchments. Catchment #07, #08, #10, and #13 show a lower parameter stability. The calculated standard deviation of the



daily NSE values shows the ranges of uncertainty provided from the simulation for the selected parameter ranges (Table S3). In this regard, catchments #08, #13, and #15 result in the lowest simulation uncertainty during calibration.



270 Figure 3: (a) The ranges of daily NSE values derived from the confined parameter sets during calibration and the corresponding NSE ranges during the validation period; and (b) the monthly aggregated NSE derived from best parameter sets from calibration, validation, and stable parameter sets for each catchment, excluding poorly performing catchments #06 and #12.

Figure 4 shows the variability of the confined model parameters obtained by the calibration, which is later applied to derive the weights of the regional regression model. The confined ranges of model parameters ( $K_0$ ,  $M_{MAXBAS}$ , and  $V_{UZL}$ ) result in a relatively uniform distribution in its median values for all catchments, except for catchments #05, #08, #13, and #15. The parameters in these catchments remained insensitive. These catchments show a narrow range of predictions for all parameters except  $M_{MAXBAS}$ . Parameters  $\beta$ ,  $F_C$ , and  $K_I$  have shown variable responses in all catchments than the remaining parameters.

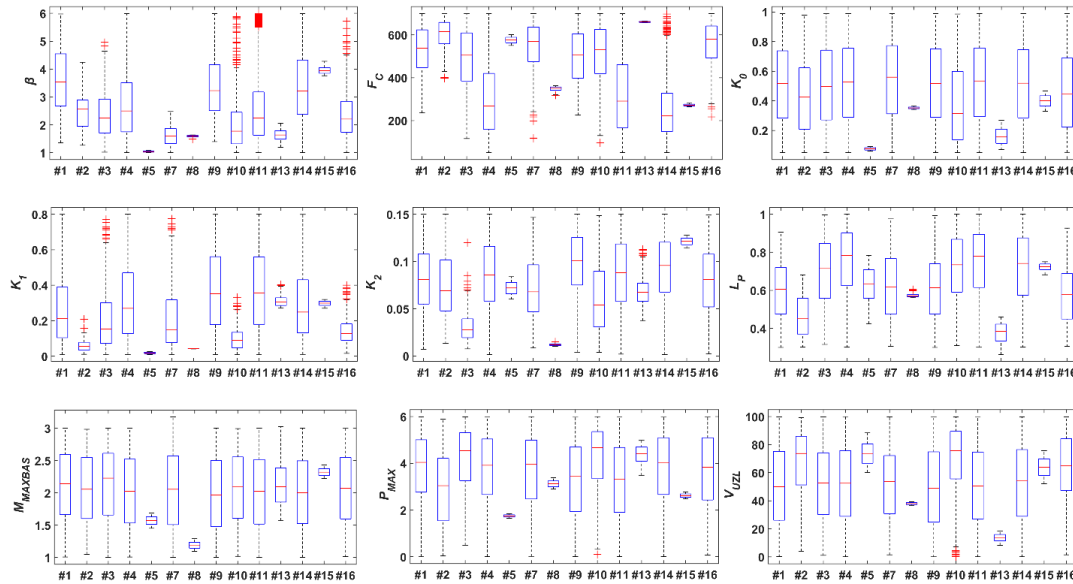


Figure 4: Confined ranges of model parameters derived during model calibration for each catchment, excluding the poorly  
 280 performing catchments #06 and #12.

#### 4.2 Performance of the regionalization procedure

We evaluate the transferability of model parameters derived from weighted regression using the Leave-One-Out method for each of the 14 gauged catchments. Figure 5a shows the scatter of monthly NSE values during the validation period obtained from the regionalized parameter sets and best parameters estimated from calibration, validation, and the most stable parameter sets. We find that regional parameter sets developed from the best validation parameters show the best performance in  
 285 predicting discharge in the left-out catchments (NSE REG<sub>val</sub> in Fig. 5b). Our results show 11 out of 14 catchments exceed a 0.25 NSE value and 7 out of 14 catchments exceed a 0.5 NSE value for the regression model derived from the validated parameters (Fig. 5a yellowish scatters). Furthermore, the median NSE value of the 14 catchments for the regression model derived from the best-validated parameters (NSE REG<sub>val</sub>) is 0.56, compared to 0.48 for the best calibration ones (NSE REG<sub>cal</sub>)  
 290 and 0.53 for the most stable parameter sets (NSE REG<sub>stable</sub>) (Fig. 5b and Table S4).

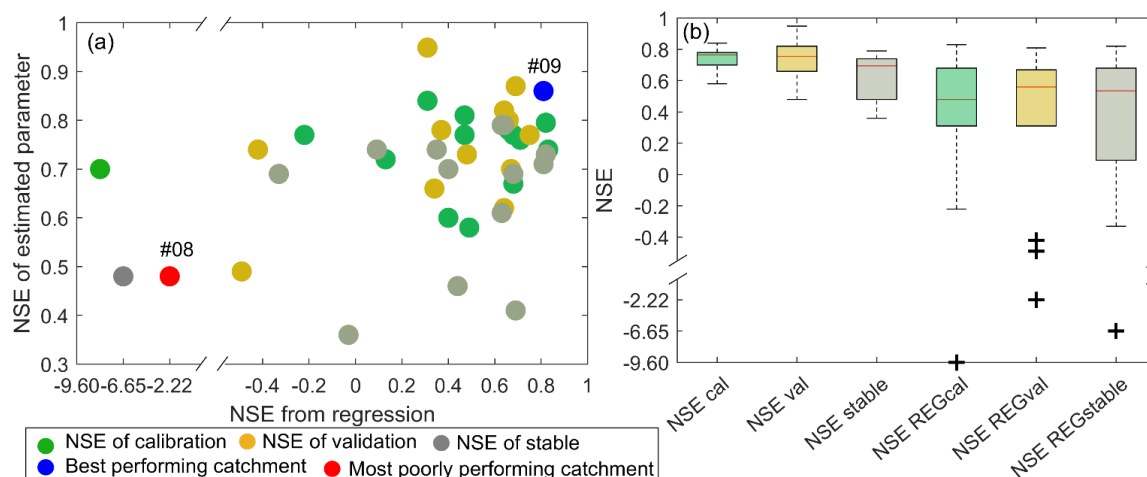


Figure 5: (a) The scatter plot of NSE for parameter estimates (from calibration, validation, and stable parameters set) compared to the NSE of parameters from the regression; and the NSE for best performing catchment (blue) and most poorly performing catchment (red) from validation. (b) The corresponding ranges of NSE obtained from the best parameter estimation (from calibration, validation, and stable sets) and ranges of NSE for parameter sets derived from the regression model (REGcal, REGval, and REGstable).

Figure 6 shows the relationships between the best model parameter set obtained from the validation and the regression for the 14 catchments. The weighted regression shows acceptable performance in reproducing most of the parameters. For instance, the weighted regression reproduces well the parameters  $\beta$ ,  $F_C$ ,  $K_0$ , and  $K_2$ , whereas the parameters located far from the 1-1 line are considered less reproducible by regression models. We notice that the weighted regression procedure does not always produce model parameters in their predefined range (Table 3). For example, the regressed  $F_C$  of catchment #15 is below the minimum threshold of 50. In such cases, the outlier model parameter is assigned to its minimum values. Similarly for model parameters  $K_0$ ,  $K_I$ , and  $P_{MAX}$ , some of the catchments result out of their range, and are therefore set to their minimum or maximum values. Among the remaining parameters, most of them show acceptable correlations. However, some of them, such as  $F_C$ ,  $K_I$ , and  $P_{MAX}$ , are poorly reflected through the regional regression in a few catchments. For instance,  $F_C$  in catchment #15 is poorly modeled, or this catchment is poorly identifiable by the parameter  $F_C$ . The other model parameter is  $K_I$ , where the regression model poorly represents three catchments (#07, #10, and #13). These three catchments have parameter values below the minimum range of 0 for  $K_I$ . This shows that catchments #07, #10, and #13 are not identifiable by the parameter  $K_I$ . Furthermore, catchment #08 is most poorly identified by the regionalized model parameter  $P_{MAX}$ . However, the weighted regression procedure sufficiently represents the remaining catchments. We also show the best performing (#09) and most poorly performing (#08) catchments labeled by blue and red colors, respectively. Catchment #09 primarily shows a stable prediction for all parameter-sampling procedures during calibration, validation, and stable relationships. Identifiable parameters in this catchment are also reproduced well from the regression model. Catchment #09 (blue scatter) is highly identifiable during parameter estimation, and the resulting parameters from the regression model are highly reproduced. Whereas catchment #08 (red scatter), shows poor parameter estimation results and poorly reproduced by the regression model.

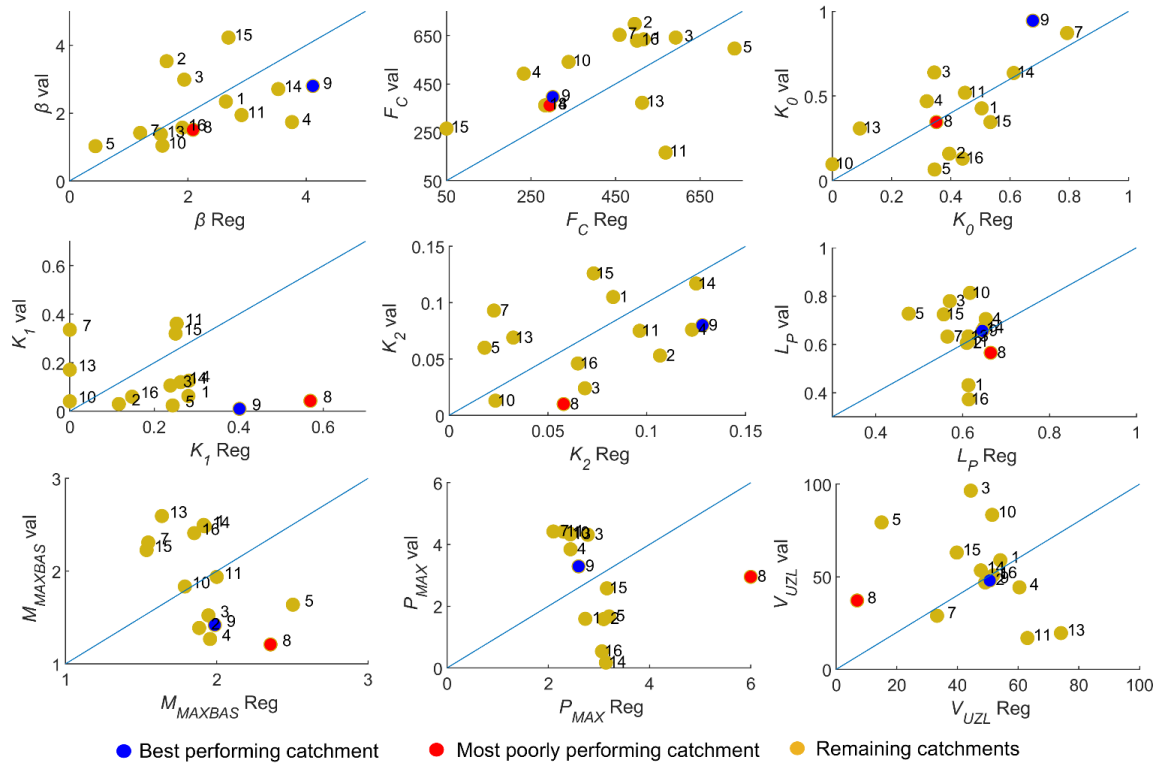


Figure 6: Scatter plots between best parameters estimated from validation and parameters derived from the regression model. The blue circle (catchment #9) represents the highly identifiable (best performing) catchment and its corresponding parameters from regression. The red circle (catchment #8) represents the (most poorly identified) catchment during parameter estimation and its corresponding regression parameters.

The reliability of our approach is further evaluated by comparing the observed discharge with the uncertainty interval of the regionalized model while running the model for the validation period (Fig. 7). Observed discharge for the best performing catchment (#09) is bounded in the prediction interval through the low flow and high flow periods. Furthermore, it corresponds highly with the mean of the 14 regionalized simulations (Fig. 7a). Whereas the observed discharge for the most poorly performing catchment (#08) is not well captured by the prediction interval nor by the mean of the 14 regionalized simulations (Fig. 7b).

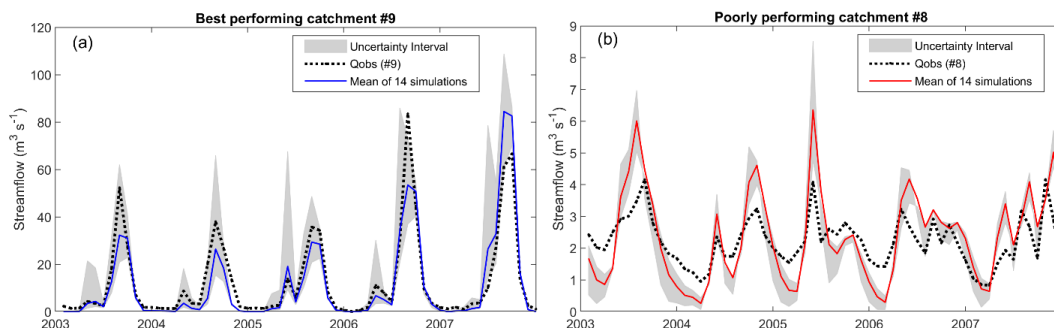




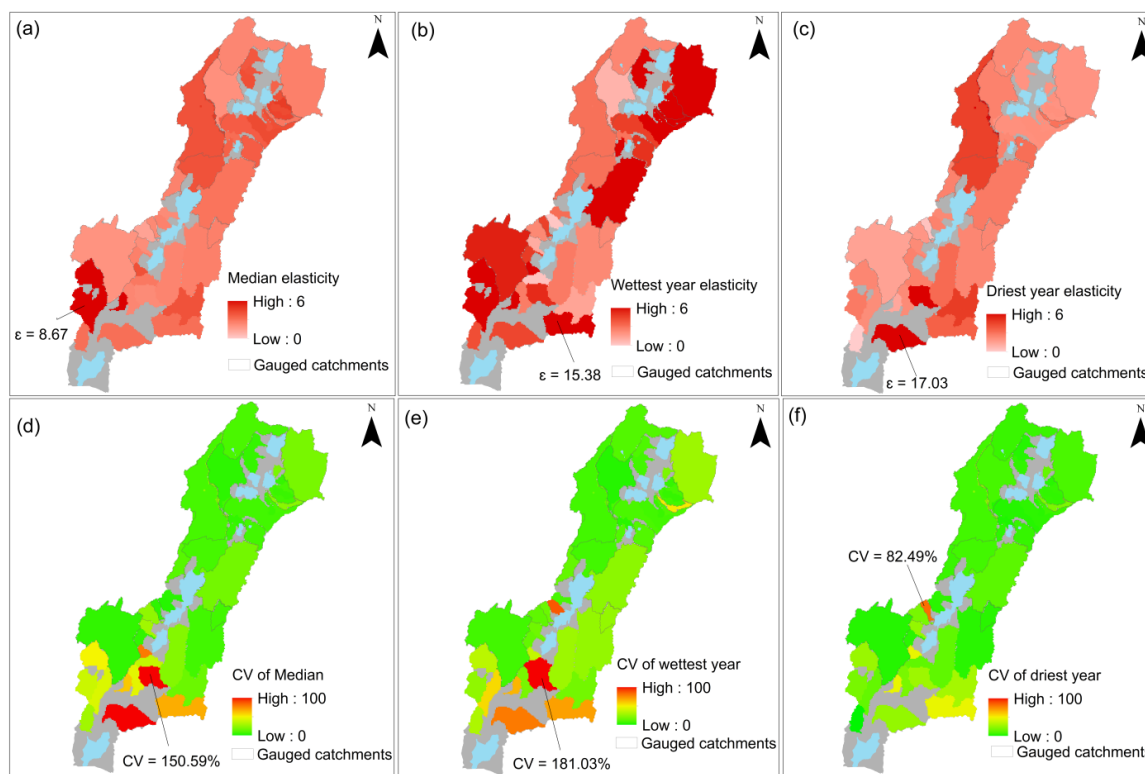
Figure 7: Prediction interval derived from the 14 regression models using best parameter sets from validation and uncertainty interval; (a) for best performing catchment (#09) and mean of the 14 simulations (blue color), and (b) uncertainty interval for  
 330 most poorly performing catchment (#08) and mean of the 14 simulations (red color).

#### 4.3 Estimation of regional resilience of streamflow to precipitation variability

With the acceptable performance of the regional regression model, we apply the model for the ungauged catchments over the entire RVLB region. Figure 8 shows the median, wettest, and driest year elasticities computed from both gauged (all parameter combinations with  $NSE \geq 0.5$ ) and ungauged catchments (all 14 regionalized parameter sets from the Leave-One-Out  
 335 evaluation). Median elasticity values are fairly distributed in the basin. However, the highest elasticity is shown in the southwest (Fig. 8a). For the wettest year, the highest elasticity results from the catchments in the south and the northeast that show less resilience for extreme precipitation (Fig. 8b). Relatively low elasticities result from the driest year, except for few catchments in the south. This variation is because catchments in the south, except for some outliers, are mainly dry and receive a comparatively low amount of precipitation.

340 With the CV, we show the uncertainty of the 14 ensembles derived from the regression. We see that the median values, as well as the wettest and driest year elasticities, show low uncertainty in the gauged catchments, indicated by low CVs (Fig. 8d–f), compared to the ungauged regions. Whereas the highest CV values are shown for the median, wettest, and driest years for the ungauged catchments in the southern region. However, most of the catchments in the central and northern parts show less variability, which shows low uncertainties for these catchments. The highest and lowest precipitation will eventually result in  
 345 different values of elasticities. In areas like RVLB, the highest yearly and seasonal precipitation amounts could be interrupted by the seasonal or yearly dry spells (Segele and Lamb, 2005). The response to runoff is low in the driest year as shown by low elasticity values in most of the ungauged catchments (Fig. 8c). Comparatively, the driest year CV in the southern part shows relatively lower values than the wettest year.





350 Figure 8: (a-c) Elasticity calculated for the median, wettest, and driest years for both gauged and ungauged catchments, and (d-f) their corresponding simulation uncertainty expressed by the coefficient of variation CV.

## 5 Discussion

### 5.1 Reliability of the regionalization approach

Our study demonstrates the applicability of a process-based hydrological model at a regional scale despite data scarcity. We show the reliability of our entire approach through a three-step parameter estimation and model evaluation procedure, which enables us to identify the most reliable setting in the regional model development procedure. Overall, the stability of parameters for the calibration and validation periods remained acceptable. We quantify uncertainty by parameters sampled from the Monte Carlo random sampling procedure. We applied the split sampling test to select the best parameter from the calibration and validation periods. Furthermore, we calculated the most stable parameter sets from the calibration and validation periods, which has also been done in previous studies aiming at stable predictions (Hartmann et al., 2016). The stability of model parameters indicates a relatively uniform system response from both calibration and validation. With an average decrease of 0.40 % from calibration to validation, our findings are similar to studies showing the decline during the validation period performance relative to the calibration period in the Conceptual Rainfall Runoff (CRR) model (Bastola et al., 2011; Coron et al., 2012).

We estimated parameters for the ungauged regions through the weighted regression procedure. Like previous studies using a similar approach (Wagner and Wheeler, 2006), the weighting procedure increases the representation of identifiable parameters



from the catchment in the regression model. More weight (reciprocal of CV) is assigned for the more identifiable parameters in a given catchment. Consequently, a three-regression model is derived from the best parameter sets obtained from calibration, validation, and stable parameter sets, enabling us to choose the optimum regional model. These procedures increase the reliability of our approach for model development. We also quantify uncertainty through the spatial cross-validation of parameters. In this approach every catchment is considered as an evaluation catchment, while prediction is made using the remaining catchments. Therefore, 14 catchments produced a 14-regression model in the Leave-One-Out method that quantifies prediction uncertainty in the ungauged catchments. The spatial cross-validations also show better performance in the regionalization studies that use discharge signatures (Zhang et al., 2018). This method is more stable and more resilient to errors that emerge from parameter sampling, and it provides a comprehensive evaluation of prediction skills for the few numbers of catchments used (Hastie et al., 2005). The spatial cross-validation approach also has a uniformly low bias and root mean squared error (RMSE) (Breiman and Spector, 1990). Therefore, we combine three steps of uncertainty quantification from 1) the parameter sampling, 2) the best parameter set identification, and 3) the spatial cross-validation in the data-scarce regions.

A scatter plot of monthly NSE between parameters estimated and parameters regionalized shows the evaluation and reliability check. Figure 5a indicates that regression parameters from the validation outperform the parameters obtained from calibration and stable sets in most of the catchments applied for cross-validation. Furthermore, it shows most of the scatter points are above a 0.5 limit, indicating a better reproduction of parameters. In this regard, parameters in 50 % of the catchments result in  $NSE \geq 0.5$  and in 79 % of the catchments,  $NSE > 0$ , for the regression model derived from the validated parameters (Fig. 5a). The median value of NSE for the 14 catchments is 0.56; this is a sufficient performance in regionalization despite the few catchment numbers applied (Fig. 5b). Figure 6 shows that more identifiable parameters for the gauged catchments (Fig. 4) are also reproduced well from the regression model. Catchment #09 (blue scatter) is highly identifiable during parameter estimation and the resulting parameters from the regression model are highly reproduced. Whereas catchment #08 (red scatter) shows poor parameter estimation results and is poorly reproduced by the regression model. Studies also show the selection of more identifiable catchment as a donor for parameter regionalization depends on the score during parameter calibration and validation (Beck et al., 2016).

In general, our evaluation indicates that despite ignoring parameter interactions (Bárdossy, 2007; Brunner et al., 2018), our regionalization procedure produces useful predictions of the model parameters in the ungauged catchments. Plotting the simulated (monthly) time series of the best and the most poorly performing regional catchments (Fig. 7), we show that the uncertainty estimates derived from the Leave-One-Out procedure capture well the simulation uncertainty for the best performing catchment #09 (blue color). On the other hand, the prediction interval of catchment #08 shows less agreement with observed discharge, particularly for low flow and high flow, but with the estimated ranges of uncertainty much closer to the observations. Previous regionalization studies have already shown that some outlier catchments cannot be captured if they behave very differently from the general trend (Seibert, 1999), as it is most probably the case for catchment #08. However, since most regionalized catchments with  $NSE \geq 0.5$ , we have reason to believe that the parameters of most ungauged catchments in the RVLB can be approximated acceptably.

## 5.2 Parameter sensitivity and spatial variability

We find different sensitivities of model parameters among our gauged catchments (Fig. 4). Since the hydrogeology of the



region is very heterogeneous, parameters controlling the underground water flow show high variabilities across the catchments. Volume controlling parameters ( $\beta$ ,  $F_C$ , and  $L_P$ ) are found to be highly identifiable in most of the catchments. Consistent with  
 405 previous studies, catchments #09 and #11 show these three parameters to be the most sensitive (Goshime et al., 2020). Catchments #01, #03, #09, and #11 are highly identifiable during parameter estimation. However, parameter insensitivity in some catchments may be due to interactions with other parameters. Abebe et al. (2010) show the interaction between parameter  $K_2$  and the percolation rate ( $P_{MAX}$ ), where the increment of  $K_2$  beyond the optimum rate of percolation may not show any sensitivity. In addition, the insensitivity of model parameters is related to the poor identifiability of model parameters in the  
 410 catchments. For instance, parameters such as  $K_0$ ,  $M_{MAXBAS}$ ,  $P_{MAX}$ , and  $V_{UZZ}$ , show high variations from the uniform ranges of parameter values for the poorly identifiable catchments (#05, #07, #08, and #10) (Fig. 4).

The most identifiable parameters in a catchment result in the highest sensitivity towards any parameter value. However, parameter insensitivity is due to variations in the values of catchment properties. This is illustrated by parameter  $M_{MAXBAS}$ , which is a transformation function or a delay in the runoff formation process, and it is well identified in catchments #13 and  
 415 #15. The shortest delay in the runoff formation process occurs due to the relatively high drainage density in these catchments (Table 2), suggesting the sensitivity of this parameter towards the lower value. Studies also show a correlation between the volume of runoff and drainage density (Di Lazzaro et al., 2015; Tague and Grant, 2004). Parameter  $P_{MAX}$  is well identified in catchments #03 and #13. The higher percolation amount directly corresponds with the highest porosity measured in these catchments (Table 2), suggesting the sensitivity of this parameter towards the higher value in the parameter range. Furthermore,  
 420 parameter  $V_{UZZ}$  is well identified in catchment #05, which has a relatively higher amount of precipitation and lower values of porosity, promoting the formation of quick flow. Generally, this causes lower values of parameter  $V_{UZZ}$  to be more sensitive to allow quick runoff formation in the catchment.

The interactions among model parameters may not be the only reason for insensitivity as it varies in different catchments and their properties. For instance, sloppy catchments in a small drainage area (#08 and #10) facilitate the conversion of precipitation  
 425 into runoff, resulting in less soil moisture in the upper and lower reservoirs in the HBV model. In such cases, adjustments to parameters ( $K_1$  and  $K_2$ ) controlling the water flow might not affect the outflow conditions. This is also shown by the negative correlation of slope with these parameters (Table S1). Furthermore, insensitivity of parameters in the upper reservoir can be affected by low precipitation amounts. In low precipitation conditions (such as in catchments #09, #11, and #15) the resulting soil moisture from the soil profile and the upper reservoir will be much less, resulting in less runoff. The adjustment of runoff  
 430 controlling parameters ( $K_0$  and  $V_{UZZ}$ ) might not have any influence (remain insensitive) on the resulting runoff. Parameter  $K_0$  only functions when the cumulative precipitation exceeds the threshold of  $V_{UZZ}$  value; therefore, higher values of  $K_0$  result in wet catchments (#10) with a higher amount of precipitation. Our study shows the insensitivity of model parameters to be related to catchment properties.

### 5.3 Estimation of regional resilience of streamflow to precipitation variability

435 We calculate elasticity values for the median, wettest, and driest years and their respective CV (Fig. 8). In the regions with higher elasticities (Fig. 8a–c), both gauged and ungauged catchments respond faster to any change in precipitation by promoting fast surface flow. However, for low elasticity values, the streamflow responds slowly to precipitation change.



The CV indicates the uncertainty of our prediction for the gauged and ungauged catchments (Fig. 8d–f). Most of the catchments located in the southern part of the basin show a higher CV value in combination with low resilience of streamflow to precipitation variability. Prediction variability is higher in the southern part compared to the north and there is also a few number of gauged catchments. So the higher uncertainty in the south may be attributable to the mixed effects of higher precipitation variability and the remoteness of the gauged catchments used to establish the regional regress.

The variability in areas of gauged and ungauged catchments used for parameter estimation and prediction, respectively, reduces with the strength of correlation between calibrated parameters and catchment properties (Table S1). Other studies also show that runoff from smaller catchments can have a stronger relationship with local climate and catchment properties than larger catchments (Bárdossy, 2007; Kokkonen et al., 2003; Merz and Blöschl, 2004). In addition, the wettest year shows higher uncertainty compared to the driest year. However, most of the ungauged catchments that are located in the central and northern parts show lower uncertainty, more or less similar to the gauged catchments. This is because these ungauged catchments are much closer to the gauged catchments and are hence better represented by the regression model than the remote ungauged catchments. Moreover, most of the streamflow in the north remains more resilient to precipitation change as it shows lower elasticity values, which indicate a higher resilience to streamflow in the dry years (Fig. 8c). Furthermore, CV for the driest year shows a relatively low uncertainty in the north for both gauged and ungauged catchments.

The application of our approach to the RVLB shows that the predicted elasticities are characterized by a wide range of uncertainty for the ungauged catchments in the southern part. The reasons for such variation in uncertainty could be the fact that the ungauged catchments in the southern part are mainly dry and receive a comparatively low amount of rainfall (Table S2). This is different from the wetter, northern part, where most of the gauged catchments are located. This accords with studies showing a decreasing regionalization performance from smaller and more arid catchments (Parajka et al., 2013). Previous work has also shown that spatial variability of precipitation can interact with catchment properties to alter hydrological processes (Zhao et al., 2013). Thus, higher precipitation variability in the gauged and ungauged catchments introduces more uncertainty to parameter regionalization. Such variability in prediction also results from the relative location of an ungauged catchment to the gauged one where the regional model is developed (Patil and Stieglitz, 2012).

This approach shows variability in the resilience of gauged and ungauged regions, which emerges from parameter uncertainty and climate variability. Over the RVLB, lakes are particularly stressed by growing water demand, climate variability, and drought (Seyoum et al., 2015). The reliability of open water resources in low-resilient catchments remains uncertain. Coupled with the significant reduction of lake sizes and water levels (Ayenew and Becht, 2008), this will negatively affect water resource availability and ecosystem stability in the future.

#### 5.4 Transferability of the approach to other catchments and models

We provide a methodology that accounts for uncertainty throughout all steps of the regionalization approach. It translates data limitations into remaining uncertainties that we find in the regional simulations (expressed, for instance, by the CV values of the elasticities). The approach is independent of the model and the number of parameters, but we expect that a more complex model (with more parameters) would struggle more through data limitations and would produce larger uncertainties when applied regionally.

In our study the identifiability of the model parameters varies across the 14 catchments. This could be from the variation in the



catchment properties used for the regionalization. Van Esse et al. (2013) show the performance of conceptual hydrological  
 475 models to vary depending on the size and soil moisture content of a catchment. In our approach this variation is accounted for  
 through regionalization uncertainties and spatial cross-validation. Thereby, one can have different levels of parameter  
 identifiability in the transferability of a model parameter from one model component to another. Nevertheless, model parameter  
 transferability does not always result in success. The difference in model parameters could derive from the complex relationship  
 between different model components within the model structures. The stability and resilience of model parameters from the  
 480 regionalization procedure would minimize the error and bias in parameter transfer within the model component (Breiman and  
 Spector, 1990). However, success in the parameter transfers will be influenced by the dominant catchment properties that are  
 identified regionally (Singh et al., 2014).

Our approach demonstrates a resilient parameter regionalization through spatial cross-validation that enables the transfer of  
 parameters across regions and within the model components in the different model structures. Other studies suggest the  
 485 applicability of spatiotemporal transfer of model parameters for climate change related studies (Patil and Stieglitz, 2015).

## 6 Conclusion

In this study we demonstrate the use of global data products for the regionalization of model parameters using a small sample  
 of gauged catchments despite data scarcity. We apply multiple options for parameter estimation and model evaluation  
 procedures. We combine three steps of uncertainty quantification from the parameter sampling, best parameter sets  
 490 identification, and spatial cross-validation. We demonstrate the validity and reliability of this approach at 14 test catchments  
 with varying catchment properties. The parameter estimates from the spatial cross-validation using the best validation  
 parameters has outperformed the parameter estimates from best-calibrated and stable parameter sets. We incorporate  
 uncertainties from the spatial cross-validation that can provide a robust way of uncertainty quantification by generating 14  
 estimates of plausible streamflow ensembles and simulation uncertainties. This approach shows variability in the resilience of  
 495 gauged and ungauged regions, which emerges from parameter uncertainty and climate variability. We show the uncertainties  
 of elasticities in the gauged catchments obtained from simulation to be less than that of the uncertainties of elasticities in the  
 ungauged catchments obtained from regionalization. The study further enables the quantification of the wettest and driest year  
 elasticities and their uncertainties throughout the catchments, which provides a basis for the integrated water resource  
 management in the region. Linking our approach with more observations of catchment properties on a larger scale can provide  
 500 a good basis for large-scale water resource management. This approach can be extended to simulate and quantify the resilience  
 of gauged and ungauged regions under climate change by quantifying the additional uncertainties emerging from climate  
 projections.

Overall, our approach provides directions for uncertainty reduction, combining global input data with local discharge  
 measurements, that result in a refinement of estimated model parameters for both gauged and ungauged catchments. Small-  
 505 scale studies that use simple models (few parameter numbers) show the transferability of the model parameters to ungauged  
 basins in data-rich conditions (Wagener and Wheeler, 2006). In extension to this, our approach provides the possibility of  
 identifying parameters of ungauged basins in data-scarce regions, including a thorough evaluation and uncertainty  
 quantification procedure. As this approach is model-independent and the input data used are available globally, it can be applied  
 to any other data-scarce region where predictions of regional water availability are required.



## 510 7 Data availability

The climatic forcing data are publicly available and can be obtained via the link <http://www.gloh2o.org/mswep> for MSWEP and from <https://www.gleam.eu> for GLEAM. The streamflow data can be acquired on request from the corresponding author for research purposes.

## 8 Author contributions

515 TA conceptualized and wrote the paper, developed and applied the regional model, and analyzed and visualized the results. YL, ST, and AH provided supervision and advice throughout the development and application of this study and provided support in developing the manuscript.

## 9 Competing interests

The authors declare that they have no conflict of interest.

## 520 10 Acknowledgments

Tesfalem Abraham was supported by the German Academic Exchange Service DAAD and Hawassa University under the EECBP Home Grown PhD Scholarship Programme. Yan Liu and Andreas Hartmann were supported by the Emmy-Noether-Programme of the German Research Foundation (DFG, grant number: HA 8113/1-1; project “Global Assessment of Water Stress in Karst Regions in a Changing World”).

## 525 11 References

- Abebe, N. A., Ogden, F. L. and Pradhan, N. R.: Sensitivity and uncertainty analysis of the conceptual HBV rainfall-runoff model: Implications for parameter estimation, *J. Hydrol.*, 389(3–4), 301–310, doi:10.1016/j.jhydrol.2010.06.007, 2010.
- Abebe, T.: Geological map (scale 1:200,000) of the northern Main Ethiopian Rift and its implications for the volcano-tectonic evolution of the rift, Geological Society of America, Boulder Colorado, USA, Maps and Charts series, MCH094., 2005.
- 530 Addor, N., Nearing, G., Prieto, C., Newman, A. J., Le Vine, N. and Clark, M. P.: A Ranking of Hydrological Signatures Based on Their Predictability in Space, *Water Resour. Res.*, 54(11), 8792–8812, doi:10.1029/2018WR022606, 2018.
- Ayenew, T. T. and Becht, R.: Comparative assessment of the water balance and hydrology of selected Ethiopian and Kenyan Rift Lakes, *Lakes Reserv. Res. Manag.*, doi:10.1111/j.1440-1770.2008.00368.x, 2008.
- Bárdossy, A.: Calibration of hydrological model parameters for ungauged catchments, *Hydrol. Earth Syst. Sci.*, 11(2), 703–710, doi:10.5194/hess-11-703-2007, 2007.
- 535 Bastola, S., Murphy, C. and Sweeney, J.: Evaluation of the transferability of hydrological model parameters for simulations under changed climatic conditions, *Hydrol. Earth Syst. Sci. Discuss.*, 8(3), 5891–5915, doi:10.5194/hessd-8-5891-2011, 2011.
- Beck, H. E., van Dijk, A. I. J. M., de Roo, A., Miralles, D. G., McVicar, T. R., Schellekens, J. and Bruijnzeel, L. A.: Global-scale regionalization of hydrologic model parameters, *Water Resour. Res.*, 52(5), 3599–3622, doi:10.1002/2015WR018247, 2016.
- 540 Beck, H. E., Wood, E. F., Pan, M., Fisher, C. K., Miralles, D. G., Van Dijk, A. I. J. M., McVicar, T. R. and Adler, R. F.: MSWep v2 Global 3-hourly 0.1° precipitation: Methodology and quantitative assessment, *Bull. Am. Meteorol. Soc.*, 100(3), 473–500, doi:10.1175/BAMS-D-17-0138.1, 2019.
- 545 Bergström, S.: The HBV model - its structure and applications, *Swedish Meteorol. Hydrol. Institute, Norrköping*, 4(4), 1–33, 1992.
- Beven, K.: A manifesto for the equifinality thesis, *J. Hydrol.*, 320(1), 18–36, doi:https://doi.org/10.1016/j.jhydrol.2005.07.007, 2006.





- Beven, K.: Environmental modelling: An uncertain future?, 2018.
- 550 Blöschl, G., Sivapalan, M., Wagener, T., Viglione, A. and Savenije, H.: Runoff prediction in ungauged basins: Synthesis across processes, places and scales., 2011.
- Breiman, L. and Spector, P.: Submodel Selection and Evaluation in Regression. The X-random, , 1989(197), 1990.
- Brunner, M. I., Furrer, R., Sikorska, A. E., Viviroli, D., Seibert, J. and Favre, A. C.: Synthetic design hydrographs for ungauged catchments: a comparison of regionalization methods, Springer Berlin Heidelberg., 2018.
- 555 Coron, L., Andréassian, V., Perrin, C., Lerat, J., Vaze, J., Bourqui, M. and Hendrickx, F.: Crash testing hydrological models in contrasted climate conditions: An experiment on 216 Australian catchments, Water Resour. Res., 48(5), doi:10.1029/2011WR011721, 2012.
- Döll, P., Kaspar, F. and Lehner, B.: A global hydrological model for deriving water availability indicators: model tuning and validation, J. Hydrol., 270(1), 105–134, doi:https://doi.org/10.1016/S0022-1694(02)00283-4, 2003.
- 560 Van Esse, W. R., Perrin, C., Booij, M. J., Augustijn, D. C. M., Fenicia, F., Kavetski, D. and Lobligeois, F.: The influence of conceptual model structure on model performance: A comparative study for 237 French catchments, Hydrol. Earth Syst. Sci., 17(10), 4227–4239, doi:10.5194/hess-17-4227-2013, 2013.
- Goshime, D. W., Absi, R., Haile, A. T., Ledésert, B. and Rientjes, T.: Bias-Corrected CHIRP Satellite Rainfall for Water Level Simulation, Lake Ziway, Ethiopia, J. Hydrol. Eng., 25(9), 05020024, doi:10.1061/(asce)he.1943-5584.0001965, 2020.
- 565 Hartmann, A., Kobler, J., Kralik, M., Dirnböck, T., Humer, F. and Weiler, M.: Model-aided quantification of dissolved carbon and nitrogen release after windthrow disturbance in an Austrian karst system, Biogeosciences, 13(1), 159–174, doi:10.5194/bg-13-159-2016, 2016.
- Hastie, T., Tibshirani, R. and Friedman, J.: The Elements of Statistical Learning : Data Mining , Inference and Prediction Probability Theory : The Logic of Science The Fundamentals of Risk Measurement Mathematicians , pure and applied , think
- 570 there is something weirdly different about, Math. Intell., 27(2), 83–85 [online] Available from: <http://link.springer.com/article/10.1007/BF02985802?LI=true#>, 2005.
- Hundecha, Y. and Bárdossy, A.: Modeling of the Effect of Land Use Changes on the Runoff Generation of a River Basin Through Parameter Regionalization of a Watershed Model, J. Hydrol., 292, 281–295, doi:10.1016/j.jhydrol.2004.01.002, 2004.
- 575 Huscroft, J., Gleeson, T., Hartmann, J. and Börker, J.: Compiling and Mapping Global Permeability of the Unconsolidated and Consolidated Earth: GLobal HYdrogeology MaPS 2.0 (GLHYMPS 2.0), Geophys. Res. Lett., 45(4), 1897–1904, doi:10.1002/2017GL075860, 2018.
- Jin, X., Xu, C., Zhang, Q. and Chen, Y. D.: Regionalization study of a conceptual hydrological model in Dongjiang basin, south China, Quat. Int., 208(1), 129–137, doi:https://doi.org/10.1016/j.quaint.2008.08.006, 2009.
- 580 Kapangaziwiri, E., Hughes, D. A. and Wagener, T.: Incorporating uncertainty in hydrological predictions for gauged and ungauged basins in southern Africa, Hydrol. Sci. J., 57(5), 1000–1019, doi:10.1080/02626667.2012.690881, 2012.
- Klemeš, V.: Operational testing of hydrological simulation models, Hydrol. Sci. J., 31(1), 13–24, doi:10.1080/02626668609491024, 1986.
- Kokkonen, T. S., Jakeman, A. J., Young, P. C. and Koivusalo, H. J.: Predicting daily flows in ungauged catchments: model regionalization from catchment descriptors at the Coweeta Hydrologic Laboratory, North Carolina, Hydrol. Process., 17(11), 2219–2238, doi:10.1002/hyp.1329, 2003.
- 585 Di Lazzaro, M., Zarlenga, A. and Volpi, E.: Hydrological effects of within-catchment heterogeneity of drainage density, Adv. Water Resour., 76, 157–167, doi:10.1016/j.advwatres.2014.12.011, 2015.
- Te Linde, A., Hurkmans, R. and Eberle, M.: Comparing model performance of two rainfall-runoff models in the Rhine basin using different atmospheric forcing data sets, Hydrol. Earth Syst. Sci., 12(3), 943–957, doi:10.5194/hess-12-943-2008, 2008.
- 590 Livneh, B. and Lettenmaier, D. P.: Regional parameter estimation for the unified land model, Water Resour. Res., 49(1), 100–114, doi:10.1029/2012WR012220, 2013.
- Martens, B., Miralles, D., Hans, L., van der Schalie, R., de Jeu, R., Fernández-Prieto, D., Beck, H., Dorigo, W. and Verhoest, N.: GLEAM v3: Satellite-based land evaporation and root-zone soil moisture, Geosci. Model Dev., 10, doi:10.5194/gmd-10-1903-2017, 2017.
- 595 Masih, I., Uhlenbrook, S., Maskey, S. and Ahmad, M. D.: Regionalization of a conceptual rainfall-runoff model based on similarity of the flow duration curve: A case study from the semi-arid Karkheh basin, Iran, J. Hydrol., 391(1), 188–201, doi:https://doi.org/10.1016/j.jhydrol.2010.07.018, 2010.
- Merz, R. and Blöschl, G.: Regionalisation of Catchment Model Parameters, J. Hydrol., 287, 95–123, doi:10.1016/j.jhydrol.2003.09.028, 2004.
- 600 Nash, J. E. and Sutcliffe, J. V.: River flow forecasting through conceptual models part I - A discussion of principles, J. Hydrol., doi:10.1016/0022-1694(70)90255-6, 1970.
- Nijssen, B., O'Donnell, G. M., Lettenmaier, D. P., Lohmann, D. and Wood, E. F.: Predicting the Discharge of Global Rivers, J. Clim., 14(15), 3307–3323, doi:10.1175/1520-0442(2001)014<3307:PTDOGR>2.0.CO;2, 2001.
- 605 Parajka, J., Blöschl, G. and Merz, R.: Regional calibration of catchment models: Potential for ungauged catchments, Water Resour. Res., 43(6), 1–16, doi:10.1029/2006WR005271, 2007.



- Parajka, J., Viglione, A., Rogger, M., Salinas, J. L., Sivapalan, M. and Blöschl, G.: Comparative assessment of predictions in ungauged basins-Part 1: Runoff-hydrograph studies, *Hydrol. Earth Syst. Sci.*, 17(5), doi:10.5194/hess-17-1783-2013, 2013.
- Patil, S. and Stieglitz, M.: Controls on hydrologic similarity: Role of nearby gauged catchments for prediction at an ungauged catchment, *Hydrol. Earth Syst. Sci.*, 16(2), 551–562, doi:10.5194/hess-16-551-2012, 2012.
- Patil, S. D. and Stieglitz, M.: Comparing spatial and temporal transferability of hydrological model parameters, *J. Hydrol.*, 525, 409–417, doi:10.1016/j.jhydrol.2015.04.003, 2015.
- Pizzi, A., Coltorti, M., A. B., Disperati, L., G. S. and Salvini, R.: The Wonji fault belt (Main Ethiopian Rift): Structural and geomorphological constraints and GPS monitoring, in *Geological Society, London, Special Publications*, vol. 259, pp. 191–207., 2006.
- Sankarasubramanian, A., Vogel, R. M. and Limbrunner, J. F.: Climate elasticity of streamflow in the United States, *Water Resour. Res.*, 37(6), 1771–1781, doi:10.1029/2000WR900330, 2001.
- Segele, Z. T. and Lamb, P. J.: Characterization and variability of Kiremt rainy season over Ethiopia, *Meteorol. Atmos. Phys.*, 89(1), 153–180, doi:10.1007/s00703-005-0127-x, 2005.
- Seibert, J.: Regionalisation of parameters for a conceptual rainfall-runoff model, *Agric. For. Meteorol.*, 98–99, 279–293, doi:10.1016/S0168-1923(99)00105-7, 1999.
- Seibert, J. and Vis, M.: Teaching hydrological modeling with a user-friendly catchment-runoff-model software package, *Hydrol. Earth Syst. Sci.*, 16, 3315–3325, doi:10.5194/hess-16-3315-2012, 2012.
- Seyoum, W. M., Milewski, A. M. and Durham, M. C.: Understanding the relative impacts of natural processes and human activities on the hydrology of the Central Rift Valley lakes, East Africa, *Hydrol. Process.*, 29(19), 4312–4324, doi:10.1002/hyp.10490, 2015.
- Singh, R., Werkhoven, K. and Wagener, T.: Hydrologic impacts of climate change in gauged and ungauged watersheds of the Olifants Basin—A trading space-for-time approach, *Hydrol. Sci. Journal/Journal des Sci. Hydrol.*, 59, 29–55, doi:10.1080/02626667.2013.819431, 2013.
- Singh, R., Archfield, S. A. and Wagener, T.: Identifying dominant controls on hydrologic parameter transfer from gauged to ungauged catchments - A comparative hydrology approach, *J. Hydrol.*, 517, 985–996, doi:10.1016/j.jhydrol.2014.06.030, 2014.
- Sivapalan, M., Takeuchi, K., Franks, S. W., Gupta, V. K., Karambiri, H., Lakshmi, V., Liang, X., McDonnell, J. J., Mendingo, E. M., O'Connell, P. E., Oki, T., Pomeroy, J. W., Schertzer, D., Uhlenbrook, S. and Zehe, E.: IAHS Decade on Predictions in Ungauged Basins (PUB), 2003-2012: Shaping an exciting future for the hydrological sciences, *Hydrol. Sci. J.*, doi:10.1623/hysj.48.6.857.51421, 2003.
- Spearman, C.: The Proof and Measurement of Association between Two Things, *Am. J. Psychol.*, 15, 72–101, doi:10.2307/1412159, 1904.
- Stokstad, E.: Scarcity of rain, stream gages threatens forecasts, *Science* (80-. ), doi:10.1126/science.285.5431.1199, 1999.
- Tague, C. and Grant, G. E.: A geological framework for interpreting the low-flow regimes of Cascade streams, Willamette River Basin, Oregon, *Water Resour. Res.*, 40(4), 1–9, doi:10.1029/2003WR002629, 2004.
- Tasker, G. D.: Hydrologic regression with weighted least squares, *Water Resour. Res.*, 16(6), 1107–1113, doi:10.1029/WR016i006p01107, 1980.
- Wagener, T. and Montanari, A.: Convergence of approaches toward reducing uncertainty in predictions in ungauged basins, *Water Resour. Res.*, 47(6), doi:10.1029/2010WR009469, 2011.
- Wagener, T. and Wheeler, H. S.: Parameter estimation and regionalization for continuous rainfall-runoff models including uncertainty, *J. Hydrol.*, 320(1–2), 132–154, doi:10.1016/j.jhydrol.2005.07.015, 2006.
- Wagener, T., Wheeler, H. S. and Gupta, H. V.: Rainfall-Runoff Modelling in Gauged and Ungauged Catchments, PUBLISHED BY IMPERIAL COLLEGE PRESS AND DISTRIBUTED BY WORLD SCIENTIFIC PUBLISHING CO., 2004.
- Westerberg, I. K., Wagener, T., Coxon, G., McMillan, H. K., Castellarin, A., Montanari, A. and Freer, J.: Uncertainty in hydrological signatures for gauged and ungauged catchments, *Water Resour. Res.*, 52(3), 1847–1865, doi:10.1002/2015WR017635, 2016.
- Widén-Nilsson, E., Halldin, S. and Xu, C.: Global water-balance modelling with WASMOD-M: Parameter estimation and regionalisation, *J. Hydrol.*, 340(1), 105–118, doi:https://doi.org/10.1016/j.jhydrol.2007.04.002, 2007.
- Woldegabriel, G., Aronson, J. L. and Walter, R. C.: Geology, geochronology, and rift basin development in the central sector of the Main Ethiopia Rift, *Bull. Geol. Soc. Am.*, 102(4), 439–458, doi:10.1130/0016-7606(1990)102<0439:GGARBD>2.3.CO;2, 1990.
- Wolfenden, E., Ebinger, C., Yirgu, G., Deino, A. and Ayalew, D.: Evolution of the northern Main Ethiopian rift: birth of a triple junction, *Earth Planet. Sci. Lett.*, 224(1), 213–228, doi:https://doi.org/10.1016/j.epsl.2004.04.022, 2004.
- Yadav, M., Wagener, T. and Gupta, H.: Regionalization of constraints on expected watershed response behavior for improved predictions in ungauged basins, *Adv. Water Resour.*, 30(8), 1756–1774, doi:10.1016/j.advwatres.2007.01.005, 2007.
- Zhang, X. and Lindström, G.: A Comparative Study of a Swedish and a Chinese Hydrological Model, *JAWRA J. Am. Water Resour. Assoc.*, 32, 985–994, doi:10.1111/j.1752-1688.1996.tb04067.x, 2007.
- Zhang, Y., Chiew, F. H. S., Li, M. and Post, D.: Predicting Runoff Signatures Using Regression and Hydrological Modeling





- 665 Approaches, *Water Resour. Res.*, 54(10), 7859–7878, doi:10.1029/2018WR023325, 2018.
- Zhang, Z., Wagener, T., Reed, P. and Bhushan, R.: Reducing uncertainty in predictions in ungauged basins by combining hydrologic indices regionalization and multiobjective optimization, *Water Resour. Res.*, 44(12), doi:10.1029/2008wr006833, 2008.
- 670 Zhao, F., Zhang, L., Chiew, F. H. S., Vaze, J. and Cheng, L.: The effect of spatial rainfall variability on water balance modelling for south-eastern Australian catchments, *J. Hydrol.*, 493, 16–29, doi:10.1016/j.jhydrol.2013.04.028, 2013.